Testing the *b*-value variability in Italy and its influence on Italian PSHA

Laura Gulia and Carlo Meletti
Istituto Nazionale di Geofisica e Vulcanologia
Via della Faggiola 32, 56126 Pisa, Italy
corresponding author: gulia@pi.ingv.it

Abstract – The supposed *b*-value spatial variability is the central topic of many scientific works dealing with forecasting modeling applications or geological correlations. If used for seismicity rates determination, the *b*-value plays an important role in probabilistic seismic hazard assessment, but how much does it influence PSHA? In the logic tree approach used for the new probabilistic seismic hazard map of Italy, named MPS04 (MPS Working Group, 2004), one of the sources of epistemic uncertainty considered was the procedure for computing seismicity rates. Two alternatives were adopted: 1) compute the activity rates for each binned magnitude class and 2) compute a Gutenberg-Richter (1944) distribution. In the logic tree branches where Gutenberg-Richter distribution was adopted, the corresponding *b*-value was evaluated for each seismogenic zone: it spans between 0.63 and 2.01.
After analysing the *b*-value variability in the Italian region, this work evaluates the impact of setting the *b*-value equal to 1 on the results of seismic hazard assessment in terms of PGA and energy release compared to the choices adopted for MPS04 (MPS Working Group, 2004).

1. Introduction

Gutenberg and Richter (1944) relation defines the empirical relationship between frequency and magnitude of earthquakes as

$$\text{Log } N(M) = a - b\,M$$

where: N is the cumulative number of earthquakes of magnitude ≥ M; *a* and *b* are constants. *a* depends on seismicity rates; *b* is representative of the earthquakes size ratio. The authors themselves define *b*-value equal to 1 on a worldwide scale and for large volumes.

Nowadays the *b*-value estimation at different scales is the subject of many scientific works, as it may reflect physical properties of the media. There are two main theories:

1. *b*-value is fixed and equal to 1 (Kagan, 2002): it implies considering the earthquake processes not only to be self-similar but also globally invariant, giving the same characteristics to small and large events;
2. *b*-value is variable (e.g. Schorlemmer et al., 2005; Schorlemmer and Wiemer, 2005; Wiemer and Schorlemmer, 2007; Shanker and Sharma, 1998; Lomnitz-Adler, 1992; Pacheco et al., 1992): it implies relationships with different tectonic regimes, stress-changes and heterogeneity of the materials.

Many authors pointed out the spatio-temporal *b*-value variability: some of them in seismic hazard assessment analysis (e.g. Shanker and Sharma, 1998, for the Himalayan region), others in earthquake forecasting modeling application (e.g. Schorlemmer et al., 2004a and 2004b, both for California) and others in correlations between *b*-value and tectonics (e.g. Lopez-Casado et al., 1995, for the Betic Cordillera; Oncel et al., 1996, for the Anatolian fault zones, Turkey; Schorlemmer et al., 2005, for a worldwide correlation between *b*-value and focal mechanisms). Bayrak et al. (2002) and Olsson (1999) summarize the state-of-the-art about the different *b*-value estimates in literature; Marzocchi and Sandri (2003) summarize different methods to estimate the *b*-value while Krinitzsky (1993) highlights the limits of the Gutenberg and Richter distribution for the application in the engineering of critical structures.

The probabilistic seismic hazard map of Italy (MPS04, MPS Working Group, 2004), recently adopted as the national reference map for planning and design purposes, was elaborated applying a logic tree approach (fig. 1) which considers two alternative sets of catalogue completeness time-intervals, four ground motion attenuation relationships (see Montaldo et al., 2005) and two different modalities for the estimation of seismicity rates: one uses the Gutenberg and Richter relation; the other evaluates independent rates for each binned magnitude class. No alternatives were considered for the seismogenic zonation (ZS9, Meletti et al., 2007; fig. 2) and for the earthquake catalogue (CPTI04, CPTI Working Group, 2004), since no really epistemic options are available. In all, the logic tree results in 16 branches which have been weighted based on expert opinion as indicated in figure1.
In the eight branches where the Gutenberg and Richter relation (from now on GR) was adopted, the *b*-value was evaluated for each seismogenic source zone yielding to values in the range from 0.63 to 2.01. Although not explicitly indicated in their technical report, the underlying assumption made by the authors of MPS04 is that the *b*-value varies as a consequence of different seismotectonic characteristics. Therefore it should vary from one source zone to the other.
To verify this hypothesis in the first part of this article we analyse the spatial variability of the *b*-value in the Italian territory at different scales using different zoning options or a regular grid.
In the second part, instead we test how a *b*-value always equal to 1 influences the seismic hazard assessment, considering all branches of the logic tree of fig.1 and the relative weights.

2. Analysis of the *b*-value spatial variability

The spatial variability of the *b*-value was analysed using a regular grid - a 16 cells square- with 1° spacing; the square vertexes are 34° N, 50° N, 5° E and 21° E (fig. 3a). We use the same catalogue adopted in MPS04, i.e. CPTI04 catalogue (CPTI Working Group, 2004) and the same two sets of completeness time-intervals, one historical and one statistical. The catalogue, developed during the processing of MPS04, contains earthquakes with $I_o \geq 5.5$ and it is declustered; only for the Etna volcanic area the threshold is lower. It reports 2550 earthquakes from 217 B.C. to 2002 A.D. in Italy and surrounding regions; moment magnitude spans between 3.92 and 7.41. Figure 4 shows the distribution of epicenters according to the two completeness time-intervals.
A difference with respect to MPS04 is that completeness intervals were defined for 12 magnitude classes and for each source zone, while we chose the completeness time-intervals of one source zone to represent an average completeness for the whole catalogue (Tab. 1), because there is not a direct correlation between source zones and cells. We calculated seismicity rates for a 100 years period for each grid cell. In order to evaluate only the impact of the fixed *b*-value, we choose to use the same procedure adopted in MPS04, including the least squares method for seismicity rates determination, even if it we are aware of its limits, as McGuire (2004) described. In CPTI04 catalogue 1471 earthquakes are consistent with historical completeness and 1113 earthquakes with the statistical one.
The *b*-value variability was evaluated through two methods: 1) by a regular subdivision of the grid in cells and 2) by grouping the cells depending on geographical neighbourhood. In this work we limited our analysis to the observation of the variability, without investigating its causes (e.g. different number of earthquakes, area dimensions or geological characteristics).

2.1 Regular subdivision of the grid

The whole grid (named *A*), which contains 256 cells, was divided into smaller areas with a decreasing number of cells: 1) half the number of cells (fig. 3b), 2) the fourth part (fig. 3c), 3) the sixteenth part (fig. 3d). The areas with *a*-value greater than 0.50 were subdivided further. Areas containing 64 to 256 cells are indicated by capital letters while smaller areas (16 cells) with capital letters and numbers and the smallest areas (4 cells; tab. 2) with capital letters, number and small letters.

Table 2 sums up the *a*-values and *b*-values obtained for successive grid subdivisions: 39 areas according to historical completeness and 38 areas according to statistical one have a statistically firm number of events. The *b*-value for the whole grid is 1.27 according to historical completeness and 1.30 according to statistical completeness (from now on first *b*-value will refer to historical completeness and the second to the statistical one). 36 areas out of 39 and 35 out of 38 (tab. 2) have a *b*-value greater than 1 and there is no correlation between the two parameters of the GR: *b*-value is independent of the number of events (fig.5). For both completenesses *b*-value shows wide variability and values much different from 1.

2.2 Geographical grouping of the cells

Cells were grouped by a rough tectonic criterion (fig. 6): North-Eastern Alps (cells 51-52-53-67-68-69-83-84), North-Western Alps (cells 54-55-56-57-70-71-72-73), Northern Apennine (cells 85-86-87-88-102-103-104), Central Apennine (cells 105-119-120-121-136-137), Southern Apennine (cells 122-138-139-140-153-154-155-156), Calabrian Arc (cells 171-172-173-187-188-189) and Sicily (cells 184-185-186-200-201-202-203-216-217-218-219). Table 3 shows the results: in the Alps, Northern Apennine, Central Apennine and Sicily the *b*-value is greater than 1 and varies from 1.15 to 1.76; in Southern Italy and Calabria it is less than 1 (from 0.93 to 0.97). These values match reasonably well the MPS04 *b*-values (tab. 4): greater than 1 for Northern and Central Italy and for Sicily, less than 1 for Southern Italy.

The above analyses, based on different kinds of subdivision of the Italian territory (cells or areas or source zones) highlight the high variability of the *b*-value: the use of a constant value seems to be unreal for the Italian region. Anyway, in order to understand if the choice of a fixed *b*-value is significant or not with respect to the seismic hazard assessment, we performed two different tests in the following.

3. Testing *b*-value equal to 1

The impact of a *b*-value fixed to 1 was evaluated through the re-processing of the whole logic tree used in MPS04 (fig. 1). We fixed the *b*-value equal to 1 in all the GR branches and selected two alternatives for the determination of *a*-value, that is the cumulative number of events:

i) ***Test 1***: the same *a*-value estimated in MPS04 was adopted, i.e. the same total number of events;
ii) ***Test 2***: re-evaluating the *a*-value in each source zones with the least squares method using the fixed b-value. As a consequence the total number of events changes with respect to MPS04: greater if the original *b*-value was less than 1; smaller in the opposite case.

As in MPS04, whenever the maximum magnitude is assumed higher than the maximum historical earthquake, the corresponding seismicity rate is determined extrapolating the GR.

Figure 7 compares the three different fitting procedures (GR distribution in MPS04 –blank circles-; GR distribution according to the test 1 approach –triangles-; GR distribution according to the test 2 approach –squares-) applied to the observed rates (i.e. cumulative number of events per magnitude bin) represented by the blank diamonds. The comparison is shown for two seismogenic source zones (SSZ) where the *b*-value computed in MPS04 was respectively greater than 1 (SSZ 915) and less than 1 (SSZ 935).

SSZ 915 (fig. 7a): test 1 has the same total number of events of MPS04 but a different distribution among magnitude classes. In particular the number of large earthquakes increases and consequently the number of small earthquakes decreases. Test 2 leads to a new *a*-value, smaller with respect to that of MPS04: the number of large earthquakes increases, while the number of small ones decreases much more than in Test 1. The seismicity rates are smaller in test 2 than in test 1 (less earthquakes are forecast).

SSZ 935 (fig. 7b): in test 1 the number of large earthquakes decreases and consequently the number of small earthquakes increases with respect to MPS04. In test 2 the new *a*-value is greater with respect to MPS04, hence the number of large earthquakes decreases, while the number of the small ones increases. Test 2 presents higher seismicity rates than test 1 (more earthquakes are forecast).

3.1 Single point and single branch analysis

Two seismic hazard maps representing PGA with 10% probability of exceedance in 50 years for hard ground sites were computed following the logic tree and the procedure described previously. In order to compare all elaborations with MPS04, the same regular spaced grid and the same software were used.

A weighted median (50th percentile) values as well as the 84th and 16th percentiles were obtained by combining the 16 individual maps in a post-processing stage as done in MPS04.

To understand how different options influence the results, we first selected and analysed two localities and compared each branch of the logic tree and the three percentiles. Results are shown in figure 8: for both localities, the single values of each branch in the tests are reported; the X axis is the PGA value and the Y axis is the relative weight of the branch. The percentiles, according to MPS04 and the two tests, are reported too. Of course, the results for the 8 unmodified branches are the same.

Fig. 8a shows the results obtained for a site in a source zone site in the northern Apennine (SSZ 915) where the *b*-value in MPS04 is greater than 1. The distribution of the points representing the 16 branches is obviously different in the three approaches. In Test 1 higher values and a wider dispersion correspond to higher median estimate and a greater variability. In Test 2, on the contrary, the median is quite similar to the MPS04 estimate.

Figure 8b shows the results obtained for a locality in a source zone in Southern Italy (SSZ 927) where the *b*-value in MPS04 is less than 1. For both tests the values obtained for single branches are lower than the MPS04 estimates and the median results are approximately 10% lower. Again in test 1 the variability increases; in test 2 it slightly decreases even if the median is lower than in MPS04.

Finally, we examined the outcomes of a single logic tree branch: in this case we show the results relative to the branch named "911" in the logic tree in figure 1, i.e. historical completeness, GR rates and Ambraseys et al. (1996) ground motion predictive relationship are the choices.

Figure 9a shows the results obtained in MPS04 for branch "911", while figures 9b and 9c represent the differences between MPS04 and test 1 and between MPS04 and test 2, respectively: in the blue areas MPS04 has PGA values lower than the test, while in the red areas MPS04 values are greater. Differences are generally more prominent in those seismogenic source zones where the original *b*-value moves away from 1, in particular:

Test 1: large negative differences are in the northern Apennine seismogenic zones (SSZ 913, 914, 915, 919, 921) and in Eolie-Patti source zone (SSZ 932), where original *b*-values are greater than 1.22; on the contrary, significant positive differences are found in southern Italy (SSZ 925, 929, 931) and in eastern Sicily (SSZ 935), where original *b*-values are less than 0.82.

Test 2: differences in PGA values are less marked than in the previous case; the largest positive differences are in the source zones 925 (*b*-values in MPS04 is 0.67) and 921 (2.00), located respectively in southern Italy and along the coast of Tuscany, while the largest negative differences are in the zones 901 (1.18) and zones 927 (0.74), located respectively in the Swiss-French border and in southern Italy. Significant differences are also present in source zones with an original *b*-value close to 1 such as in north-eastern Italy (1.06), central Apennine (1.05) and western Sicily (0.96).
As remarked for test 2 in the previous paragraph, the approach followed in this test produce a widespread decrease of the PGA values with respect to the approach adopted in MPS04.
Considering both tests, differences range between -0.084 g and +0.108 g, corresponding to a relative maximum variation of 55% and generally the approach of test 1 results in wider differences than the approach of test 2.

3.2 Median maps

The maps shown in fig. 10 represent the MPS04 (median PGA values, fig. 10a) and the differences between such map and the corresponding median PGA map obtained from test 1 (fig. 10b) and test 2 (fig. 10c). The same trend described in the previous section for the branch 911 can be observed here too, although we notice that the areas showing large maximum variations are smaller.
Differences between MPS04 and test 1: the map resulting from this approach is strictly dependent on the original *b*-values. If the original *b*-value is less than 1, PGA values are smaller than in MPS04 and if the original *b*-value is larger than 1 PGA values are greater than in MPS04. Again, the maximum variations are in those zones where *b*-values are most different from 1: minimum negative values are in the Southern (SSZ 931;original *b*-values 0.63) and Eastern Sicily (SSZ 935, original *b*-values 0.72 and 0.69); maximum positive values are in North-Eastern Italy (SSZ 906, original *b*-values 1.14 and 1.70) and in Northern Apennine (SSZs 913, 914, 915, 919; original *b*-values 1.44 - 1.80 and 1.23 – 1.70).
Differences between MPS04 and test 2: the map shows a trend similar to the map shown in figure 9c and the variations with respect to MPS04 are less evident. The source zones in eastern Sicily (SSZ 935; original *b*-values 0.72 and 0.69) and in the Adriatic sea (SSZ 931; original *b*-values 0.63) show maximum increased values, while only in North-Western Italy (SSZs 901, 902, 908, 909; original *b*-values 1.18 – 1.91 and 1.05 – 1.67) and Albani Hills (SSZ 922) show negative variations.
The differences between MPS04 and the two tests corresponds to a maximum variation of 24% (Fig. 11) limited to small areas with respect to the values in MPS04. However, since the adopted logic tree the GR branches have a smaller weight than the AR ones (40% vs 60%, fig. 1), the impact of a imposed and fixed *b*-value on SHA is smoothed in the resulting median map.

3.3 Energy release

Another way to assess the impact of a fixed and equal to 1 *b*-value is considering the energy release: different seismicity rates imply a different amount of released energy.
The energy release for MPS04 and the two tests were evaluated, both for historical and statistical completeness, in 100 years time period, by using the magnitude-energy relation from Gutenberg and Richter (1956):

$$\text{Log10 } E(\text{joule}) = 4.8 + 1.5 \text{ Ms}$$

For each source zone and for each completeness, we calculated the released energy corresponding to the magnitude of each binned class and then we multiplied it for the corresponding rates; the total energy released is the sum of the energy released for all the magnitude classes.

Table 4 shows the energy release for each source zone and for the two different sets of completeness time-intervals defined in MPS04; the *b*-values used in MPS04 are reported too. The comparison between the total energy for the different maps shows that the cumulative energy decreases with respect to MPS04 in both tests and that in test 2 the difference is more significant (9% for test 1 and 20% for test 2). In each source zone the energy release shows a direct correlation with the *b*-value: it decreases if *b*-value is less than 1, whereas it increases if the *b*-value was greater than 1. Considering the total energy (the sum of the released energy in every source zone), 29 out of 36 SSZs have *b*-value greater than 1 (the energy in the tests increases) and 7 out of 36 SSZs have *b*-value less than 1 (the energy decreases); the total energy decreases because the contribution of these latest SSZs is more than 50%.

4. Conclusions

In order to investigate new possible options for the logic tree adopted in MPS04 project (MPS Working Group, 2004), different approaches to the seismicity rates evaluations were explored, according to the current literature, where many theories on the GR distribution are presented.

In the first part of the work we estimated the *b*-value variability in the Italian territory: the values obtained confirm a wide variability of this parameter, in agreement with the *b*-values obtained for the Italian reference hazard map MPS04.

In the second part we evaluated the impact on PSHA of using a fixed *b*-value, through a comparison with MPS04: fixing *b*-value to 1, two different approaches to determine the *a*-value in GR distribution were adopted. The comparison between different approaches was performed at three levels: (1) for a single grid point, (2) for a single logic tree branch and (3) for the median PSHA map. For a single locality a general increase of variability is observed. The analysis of a single logic tree branch highlights differences in PGA values greater than in the final map: this is due to different weight of logic tree branches that determines a smoothing of variation in median values with respect to single branch values. Anyway the differences between MPS04 and the two tests corresponds to a maximum variation of 24% .

In the final part, setting the *b*-value to 1 produces a great variation in terms of energy release, that corresponds to a very different distribution of the number of earthquakes per magnitude class compared to the observed one.

In conclusion, the *b*-value in the Italian territory is extremely variable; this observation, together with the general trend observed in the tests of an increased variability of the final estimates, confirms that the use of a constant and equal to 1 *b*-value is unrealistic in this area.

Acknowledgement

This research was performed in the frame of the activities of the project S1 (one of the INGV-DPC 2004-06 applied research programs), with the financial support of the Italian Department of Civil Protection (DPC – Dipartimento della Protezione Civile).

A special thank is due to Dr. Valentina Montaldo, that since the early steps of the work encouraged us with valuable and fundamental suggestions.

The authors would also like to thank two anonymous reviewers for their useful comments which helped to improve the article.

References

Ambraseys N.N., Simpson K.A. and Bommer J.J.; 1996: *Prediction of horizontal response spectra in Europe.* Earth. Eng. Struct. Dyn., 25, 371-400.

Bayrak Y., Yilmazturk A. and Ozturk S.; 2002: *Lateral variations of the modal (a/b) values for the different regions of the world*. J. Geodyn., 34, 653-666.

CPTI Working Group; 2004: *Catalogo Parametrico dei Terremoti Italiani, versione 2004 (CPTI04)*. INGV, Bologna. http://emidius.mi.ingv.it/CPTI/

Gutenberg B. and Richter C.F.; 1944: *Frequency of earthquakes in California.* Bull. Seismol. Soc. Am., 34, 185-188.

Gutenberg B. and Richter C.F.; 1956: *Magnitudes and energy of earthquakes.* Ann. Geofis., 9, 1-15.

Kagan Y.Y.; 2002: *Seismic moment distribution revisited: I. Statistical results.* Geophys. J. Int., 148, 520-541.

Krinitzsky E.L.; 1993: *Earthquake Probability in Engineering-Part 2: Earthquake Recurrence and Limitations of Gutenberg-Richter b-values for the Engineering of Critical Structures*. Eng. Geol., 36,1-52.

Lomnitz-Adler J.; 1992: *Interplay of fault dynamics and fractal dimension in determining Gutenberg and Richter's b-value*. Geophys. J. Int., 108, 941-944.

Lopez Casado C., Sanz de Galdano C., Delgado J. and Peinado M.A.; 1995: *The b parameter in the Betic Cordillera, Rif and nearby sectors. Relations with the tectonics of the region.* Tectonophysics, 248, 277-292.

Marzocchi W. and Sandri L.; 2003: *A review and new insights on the estimation of the b-value and its uncertainty*. Ann. Geophys ., 46, 1271-1282

McGuire R.K.; 2004: *Seismic Hazard and Risk Analysis*. EERI, MNO-10, Okland, CA, page 41.

Meletti C., Galadini F., Valensise G., Stucchi M., Basili R., Barba S., Vannucci G. and Boschi E.; 2007: *The ZS9 seismic source model for the seismic hazard assessment of the Italian territory*. Submitted to Tectonophysics.

Montaldo V., Faccioli E., Zonno G., Akinci A. and Malagnini L.; 2005: *Treatment of ground-motion predictive relationships for the reference seismic hazard map of Italy.* J. Seismol., 9 (3), 295-316.

MPS Working Group; 2004: *Redazione della Mappa di Pericolosità sismica prevista dall'Ordinanza PCM 3274 del 20 marzo 2003*. Rapporto conclusivo per il Dipartimento della Protezione Civile, INGV, Milano-Roma, aprile 2004, 65 pp. + 5 appendici. http://zonesismiche.mi.ingv.it/.

Olsson R.; 1999: *An estimation of the maximum b-value in the Gutenberg-Richter relation*. Geodynamics, 27, 547-552.

Oncel A.O., Main I., Alptekin O. and Cowie P.; 1996: *Spatial variations of fractal properties of seismicity in the Anatolian fault zones.* Tectonophysics, 257, 189-202.

Pacheco J.F., Scholtz C.H. and Sykes L.R.; 1992: *Changes in frequency-size relationship from small to large earthquakes.* Nature, 355, 71-73.

Schorlemmer D. and Wiemer S.; 2005: *Microseismicity data forecast rupture area*. Nature, 434, 1086.

Schorlemmer D., Wiemer S. and Wyss M.; 2005: *Variations in earthquake-size distribution across different stress regimes.* Nature, 437, 539-542.

Schorlemmer D., Wiemer S. and Wyss M.; 2004a: *Earthquake statistics at Parkfield: 1. Stationarity of b values.* J. Geophys. Res., B12307, doi: 10.1029/2004JB003234.

Schorlemmer D., Wiemer S., Wyss M. and Jackson D.D.; 2004b: *Earthquake statistics at Parkfield: 2. probabilistic forecasting and testing.* J. Geophys. Res., B12308, doi: 10.1029/2004JB003235.

Shanker D. and Sharma M.L.; 1998: *Estimation of Seismic Hazard Parameters for the Himalayas and its Vicinity from Complete Data Files*. Pure appl. geophys., 152 , 267–279.

Wiemer S. and Schorlemmer D.; 2007: *ALM: An Asperity-based Likelihood Model for California.* Seismol. Res. Letters., 78(1), 134-140.

Figures

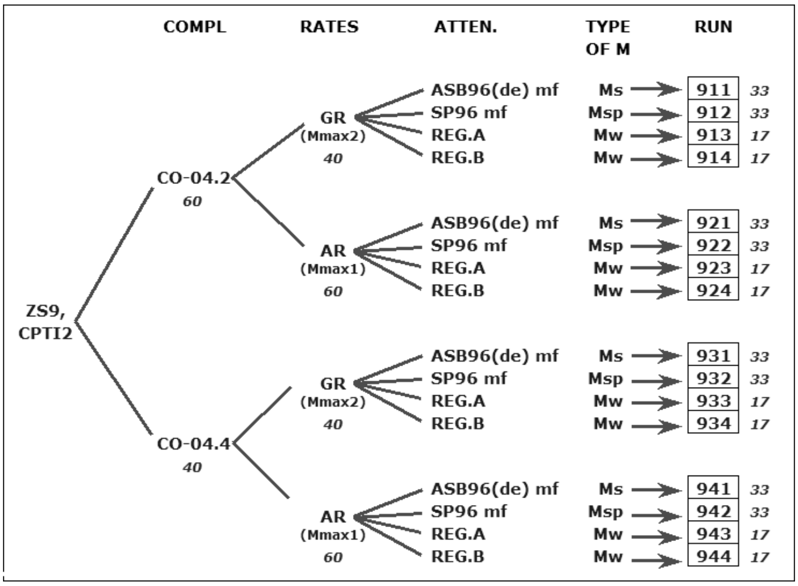

Fig. 1 - Logic tree adopted in MPS04 (MPS Working Group, 2004). The number close to each epistemic alternative represents its weight.

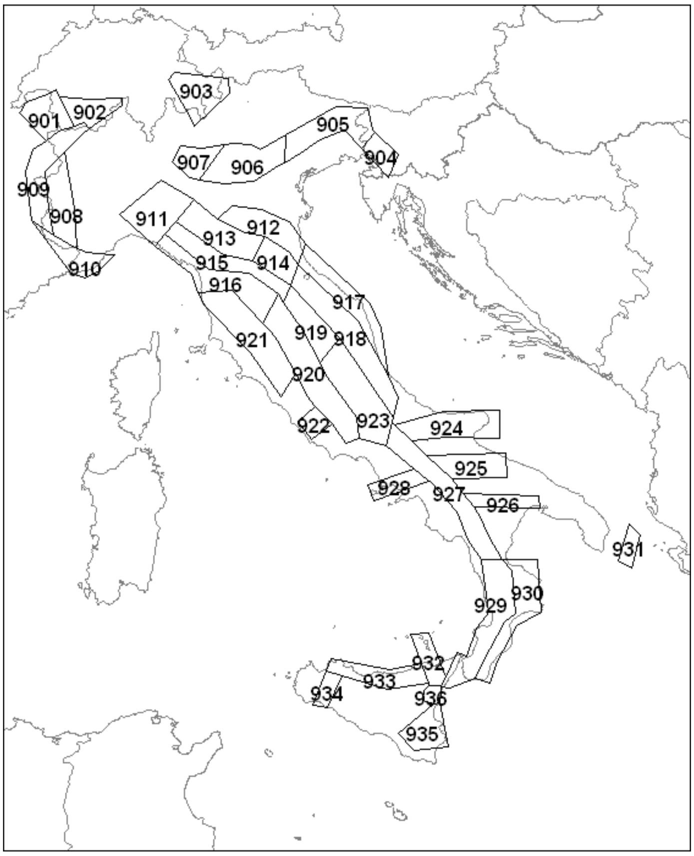

Fig. 2 – ZS9 seismogenic zonation, redrawn from Meletti et al. (2007).

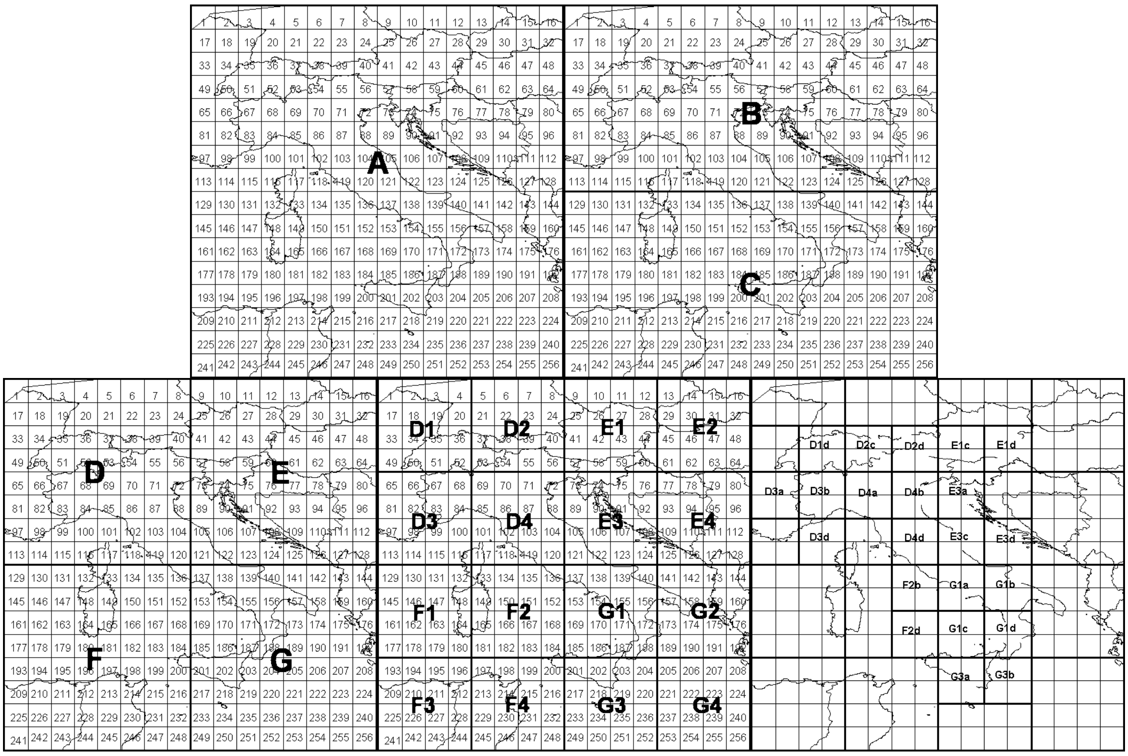

Fig. 3 - The regular grid - a 16 cells square with 1° spacing- used for the analysis of the *b*-value variability; the square vertexes are 34° N, 50° N, 5° E and 21° E. a) whole grid. Regular subdivision of the grid: b) half the number of cells; c) the fourth part; d) the sixteenth part; e) the sixtyfourth part; these areas have an *a*-value greater than 0.50.

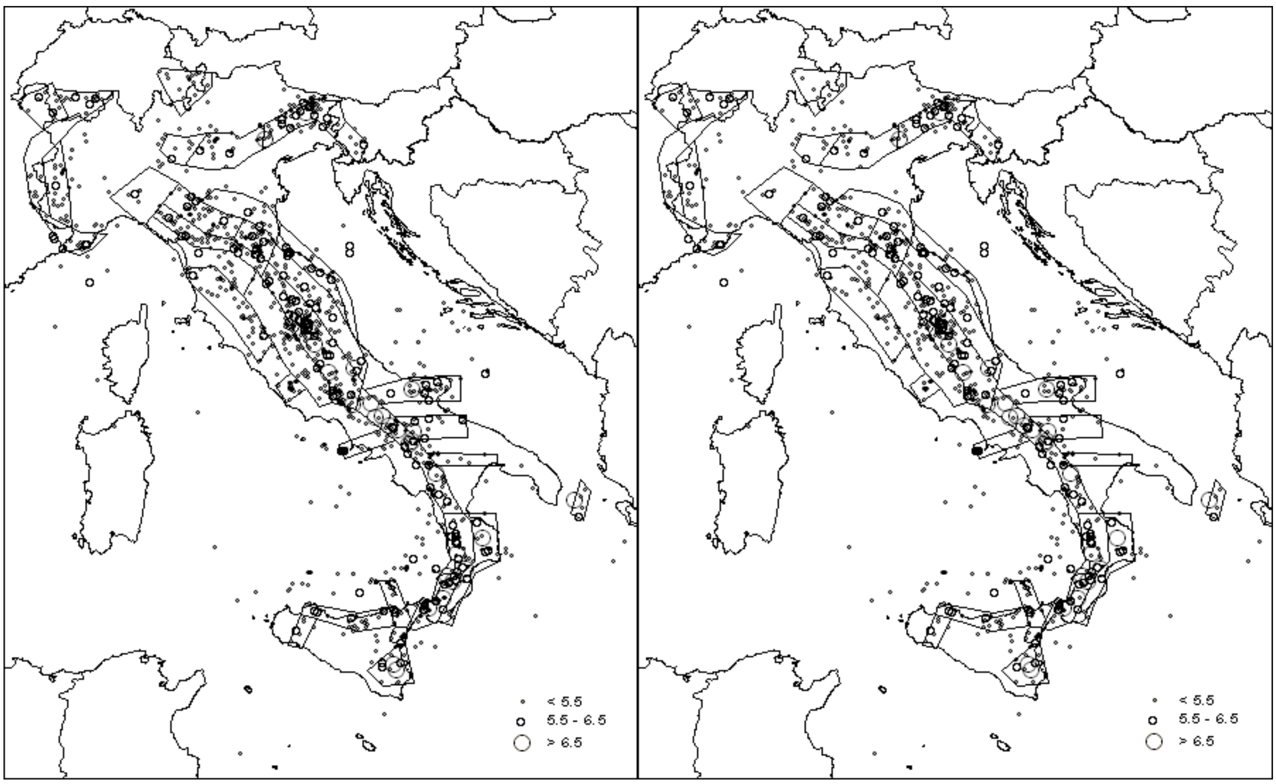

Fig. 4 – Maps of the epicenters in CPTI04, according to historical completeness time interval (a) and to statistical completeness time interval (b), showed in table 1.

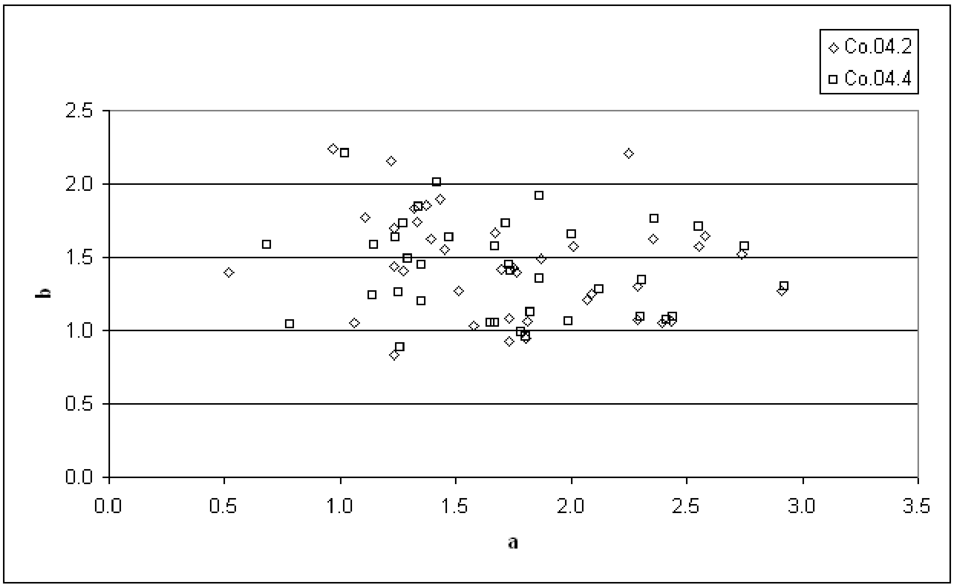

Fig. 5 – Relation between *b*-value and *a*-value (Log of the total number of earthquakes) in the whole grid and in the smaller areas, according to the historical completeness (Co.04.2) and the statistical one (Co.04.4).

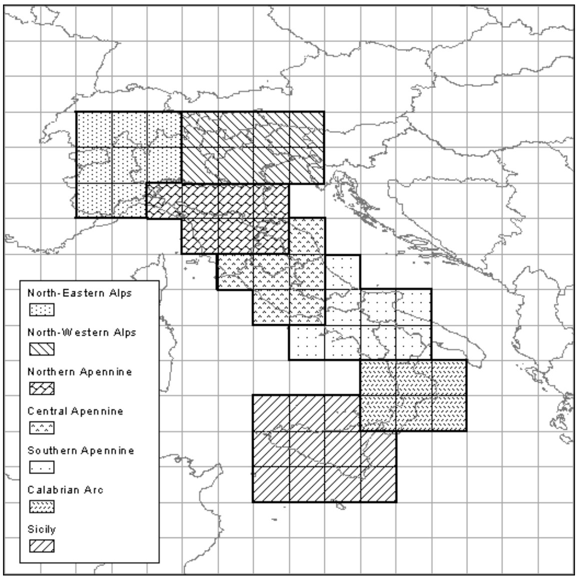

Fig. 6 - Tectonic grouping of the cells: North-Eastern Alps, North-Western Alps, Northern Apennine, Central Apennine, Southern Apennine, Calabrian Arc and Sicily.

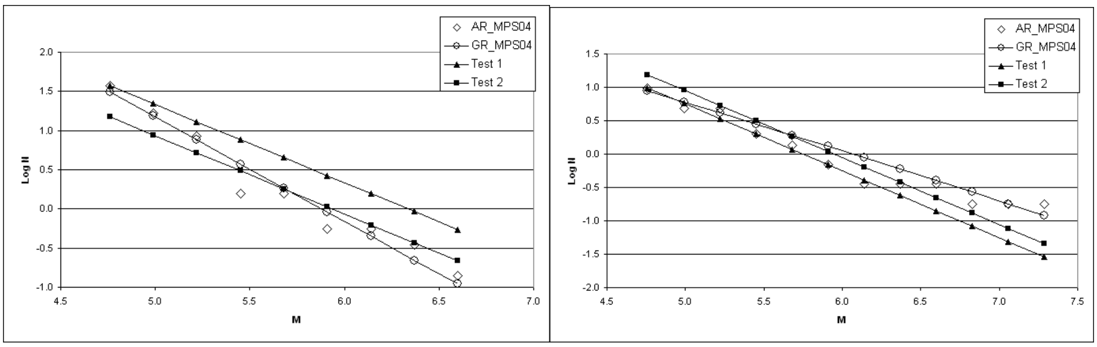

Fig. 7 - Frequency-magnitude distribution according to MPS04 (blank diamonds for AR rates and blank circles for GR rates) and the two tests (triangles for test 1 and squares for test 2): a) source zone with an original *b*-value >1 (SSZ 915); b) source zone with an original *b*-value <1 (SSZ 935).

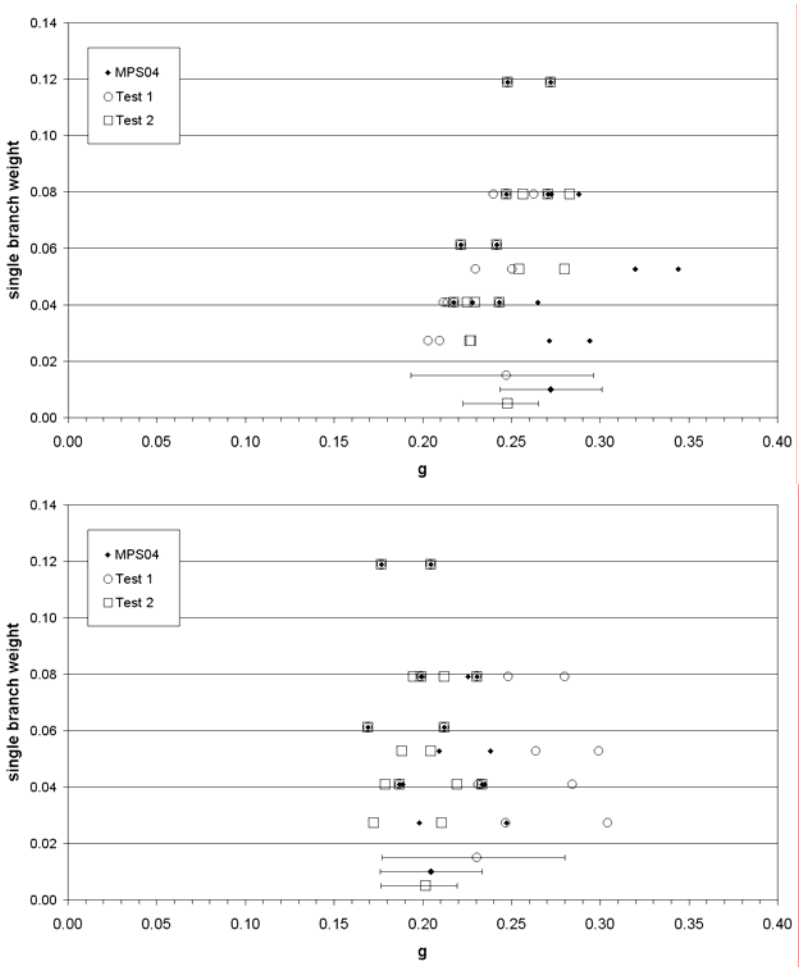

Fig. 8 - Single branch PGA values for MPS04, test 1 and test 2: a) SSZ 915; b) SSZ 935. In the lower part of the graphs the median value and the variability (expressed by the 16th and 84th percentiles) are superimposed and represented by symbol and bars.

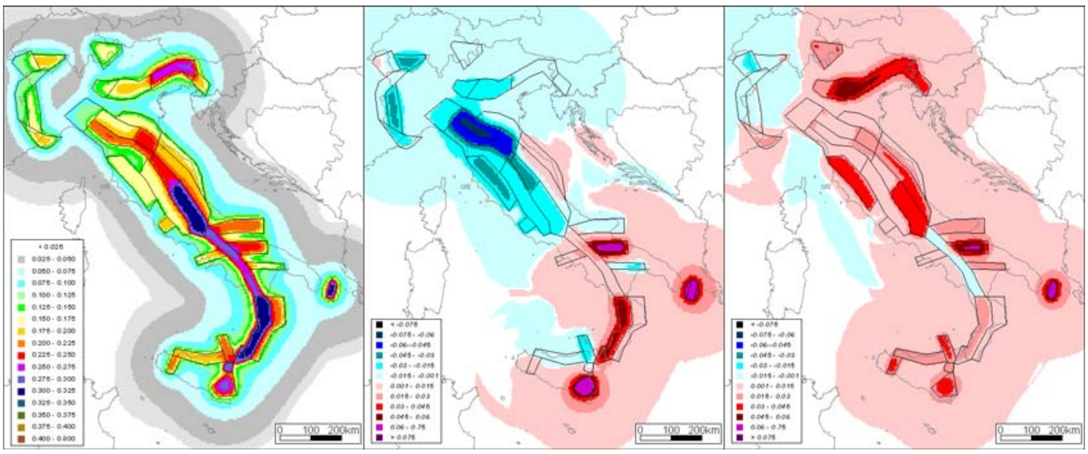

Fig. 9 - a) Map of 911 branch in MPS04; b) map of the differences between 911 branch for MPS04 and Run 911 for test 1 and c) map of the differences between 911 branch for MPS04 and Run 911 for test 2.

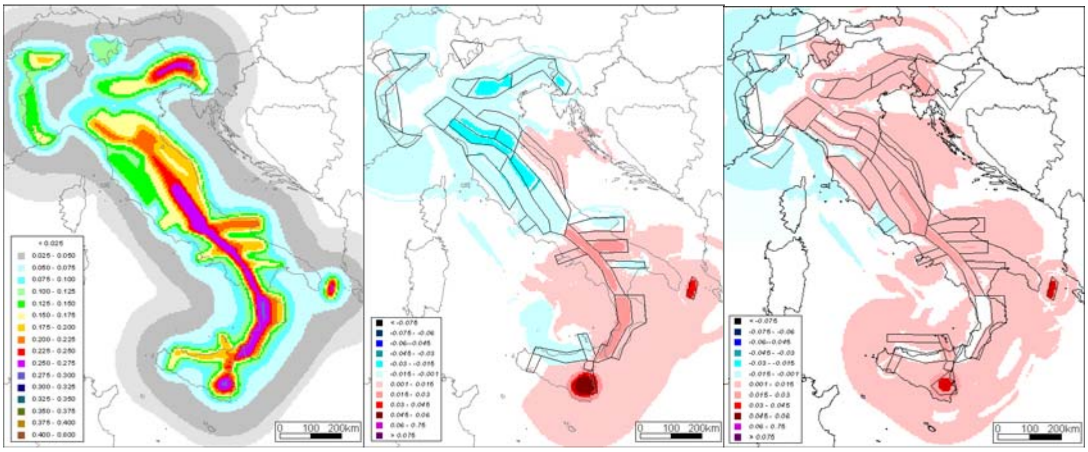

Fig. 10 - a) MPS04 median map (MPS Working Group, 2004); b) map of the differences between MPS04 median map and test 1 median map and c) map of the differences between MPS04 median map and test 2 median map.

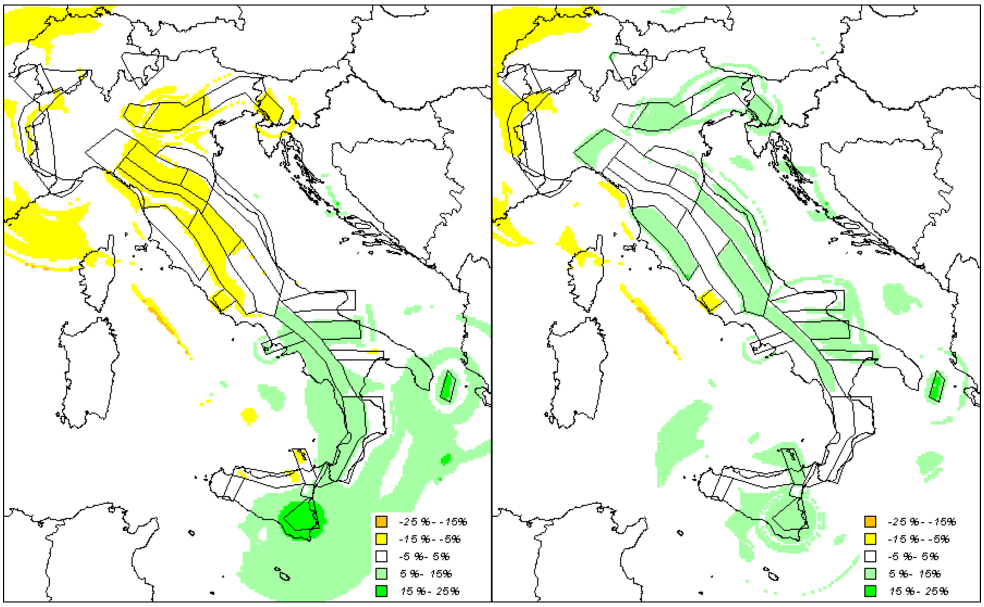

Fig. 11 - Percent different maps between MPS04 and test 1 (a) and test 2 (b).

Tables

	4.76 ±0.23	4.99 ±0.23	5.22 ±0.23	5.45 ±0.23	5.68 ±0.23	5.91 ±0.23	6.14 ±0.23	6.37 ±0.23	6.60 ±0.23	6.83 ±0.23	7.06 ±0.23	7.29 ± 0.23
Historical completeness	1871	1871	1700	1700	1530	1530	1300	1300	1300	1300	1300	1300
Statistical completeness	1910	1871	1871	1700	1700	1530	1530	1300	1300	1300	1300	1300

Table 1 – Time completeness intervals of the CPTI04 catalogue used for the analysis of the *b*-value variability in the Italian territory.

		Historical completeness		***Statistical completeness***	
Name	***Number of cells***	***a-value***	***b-value***	***a-value***	***b-value***
A	256	2.91	**1.27**	2.92	**1.30**
B	128	2.74	**1.52**	2.75	**1.57**
C	128	2.43	**1.06**	2.44	**1.09**
D	64	2.55	**1.57**	2.55	**1.71**
E	64	2.29	**1.30**	2.31	**1.34**
F	64	1.32	**1.83**	1.24	**1.64**
G	64	2.39	**1.05**	2.41	**1.07**
D1	16	1.45	**1.55**	1.35	**1.45**
D2	16	1.75	**1.43**	1.73	**1.45**
D3	16	1.70	**1.42**	1.72	**1.73**
D4	16	2.35	**1.62**	2.36	**1.76**
E1	16	1.87	**1.49**	1.86	**1.35**
E3	16	2.07	**1.21**	2.12	**1.28**
F2	16	1.23	**1.70**	1.15	**1.58**
G1	16	2.29	**1.07**	2.30	**1.09**
G2	16	1.06	**1.05**	1.99	**1.06**
G3	16	1.58	**1.03**	1.65	**1.05**
D1d	4	1.27	**1.41**	1.14	**1.24**
D2c	4	1.37	**1.85**	1.34	**1.84**
D2d	4	1.51	**1.27**	1.35	**1.20**
D3a	4	2.25	**2.21**	1.27	**1.73**
D3b	4	1.43	**1.90**	1.42	**2.01**
D3d	4	2.09	**1.25**	2.00	**1.66**
D4a	4	2.58	**1.65**	1.86	**1.92**
D4b	4	1.67	**1.67**	1.67	**1.57**
D4d	4	2.01	**1.57**	0.78	**1.04**
E1c	4	1.76	**1.40**	1.74	**1.41**
E1d	4	1.22	**2.16**	1.25	**1.26**
E3a	4	1.23	**1.44**	1.29	**1.49**
E3c	4	1.81	**1.06**	1.82	**1.13**
E3d	4	0.97	**2.24**	1.02	**2.21**
F2b	4	1.11	**1.77**	-	**-**
F2d	4	0.52	**1.40**	0.68	**1.58**
G1a	4	1.73	**1.08**	1.67	**1.05**
G1b	4	1.73	**0.93**	1.78	**0.99**
G1c	4	1.39	**1.63**	1.47	**1.64**
G1d	4	1.80	**0.95**	1.80	**0.96**
G3a	4	1.33	**1.74**	1.67	**1.05**
G3b	4	1.23	**0.83**	1.26	**0.89**

Table 2 - The *a*-values and *b*-values obtained for whole grid and for grid subdivisions according to historical and statistical completeness time intervals; each grid subdivision area is characterised by name and number of cells. Missing of some areas is due to the small number of earthquakes.

	Historical completeness		Statistical completeness	
Name	***a-value***	***b-value***	***a-value***	***b-value***
North-Eastern Alps	1.90	**1.34**	1.91	**1.28**
North-Western Alps	1.74	**1.76**	1.70	**1.66**
Northern Apennine	2.16	**1.49**	2.16	**1.64**
Central Apennine	2.19	**1.26**	2.17	**1.32**
Southern Apennine	1.89	**0.93**	1.92	**0.96**
Calabrian Arc	1.82	**0.96**	1.83	**0.97**
Sicily	1.80	**1.15**	1.88	**1.18**

Table 3 - The *a*-values and *b*-values obtained for geographical grouping of the cells.

	Historical Completeness				Statistical Completeness			
SSZ in ZS9	***MPS04 b value***	***MPS04***	***Test 1***	***Test 2***	***MPS04 b value***	***MPS04***	***Test 1***	***Test 2***
901	*1.18*	3.15	2.96	4.04	*1.26*	4.63	5.82	5.80
902	*1.26*	6.22	9.13	6.59	*1.05*	6.62	6.65	6.73
903	*1.26*	2.69	4.28	2.87	*1.05*	2.43	4.43	3.42
904	*1.12*	1.44	4.50	2.41	*1.32*	1.36	5.09	2.18
905	*1.06*	31.19	49.82	30.43	*1.12*	38.23	60.17	40.37
906	*1.14*	8.70	21.37	8.05	*1.70*	6.35	18.62	13.58
907	*1.71*	2.02	3.53	2.17	*1.48*	2.33	5.51	3.27
908	*1.91*	3.01	8.06	5.47	*1.67*	3.07	8.03	5.13
909	*1.27*	1.90	2.65	3.70	*1.38*	2.72	4.49	4.13
910	*1.12*	6.79	10.28	7.09	*1.06*	6.40	7.31	6.59
911	*1.47*	1.27	3.81	2.32	*1.33*	1.77	4.93	3.26
912	*1.35*	5.58	5.68	4.40	*1.32*	4.92	4.94	3.89
913	*1.80*	5.60	18.09	6.16	*1.53*	7.56	13.47	8.75
914	*1.33*	6.93	15.95	6.50	*1.23*	9.47	11.03	9.32
915	*1.34*	15.72	49.81	26.37	*1.36*	22.34	59.66	23.76
916	*1.96*	2.18	4.42	3.18	*1.58*	3.09	4.99	4.49
917	*1.04*	8.81	6.66	6.61	*1.01*	11.01	8.42	8.12
918	*1.10*	15.24	16.99	11.79	*1.11*	19.34	19.40	15.31
919	*1.22*	17.33	28.62	18.79	*1.39*	18.04	33.53	20.13
920	*1.96*	6.40	12.02	9.06	*1.58*	7.75	10.99	8.31
921	*2.00*	6.58	14.95	5.50	*2.01*	6.18	13.56	7.36
922	*2.00*	1.96	3.02	1.81	*2.01*	2.37	2.02	2.28
923	*1.05*	104.10	179.30	105.45	*1.09*	98.30	163.22	103.62
924	*1.04*	30.85	40.42	31.17	*1.06*	30.97	44.78	31.42
925	*0.67*	27.35	14.28	15.84	*0.75*	29.95	19.40	19.46
926	*1.28*	2.26	4.86	2.82	*1.38*	2.74	5.52	3.33
927	*0.74*	183.67	100.74	120.34	*0.72*	179.08	86.95	115.32
928	*1.04*	3.53	2.79	2.82	*0.66*	4.76	2.74	3.35
929	*0.82*	250.84	144.00	182.45	*0.79*	259.59	114.47	189.39
930	*0.98*	21.99	23.21	21.59	*0.89*	26.12	16.87	23.64
931	*0.63*	24.81	9.54	11.93	*0.63*	24.81	9.54	11.93
932	*1.21*	5.15	10.43	5.17	*1.08*	7.19	8.08	5.15
933	*1.39*	8.75	9.80	6.87	*1.24*	11.37	10.70	12.05
934	*0.96*	3.13	3.85	2.84	*0.93*	3.07	3.48	2.77
935	*0.72*	80.82	32.46	45.97	*0.69*	111.96	35.50	56.23
936	*1.63*	2.54	2.46	2.04	*1.22*	2.90	2.13	2.12
Total energy		910.51	874.74	732.61		980.78	836.42	785.93

Table 4 - Energy release (value x 10^{13} joule) in each seismogenic source zone for historical and statistical completenesses evaluated from the seismicity rates normalized to 100 years in MPS04, in the test 1 and in the test 2 and adopted *b*-values in MPS04.